Macromolecules 1993, *26*, 5755–5764

Photopolymerization of Micelle-Forming Monomers. 1. Characterization of the Systems before and after Polymerization

Didier Cochin, Françoise Candau, and Raoul Zana[*]

Institut Charles Sadron (CRM-EAHP), CNRS-ULP Strasbourg, 6, rue Boussingault, 67083 Strasbourg Cédex, France

Received March 29, 1993; Revised Manuscript Received July 19, 1993[⊛]

ABSTRACT: Cationic surfactants bearing a polymerizable styryl headgroup and a variable alkyl chain (C*n*-STY with $n = 8$, 12, and 16) have been synthesized. Their aqueous solutions have been characterized by the surfactant critical micellar concentration (cmc) and aggregation number using electrical conductivity, spectrofluorimetry, and time-resolved fluorescence quenching. The photoinitiated polymerization of these surfactants in the micellar state led to stable and transparent or slightly bluish systems. The polymerized systems poly(C*n*-STY) and the recovered polymers were characterized by means of several complementary techniques. The polymers have high molecular weights (3×10^5–3×10^6) which indicate that the initial micellar structure is not preserved upon polymerization. The structure of the polymerized systems depends on the alkyl chain length of the surfactant. The poly(C16-STY) systems exhibit a structure similar to that of a polysoap with intramolecular hydrophobic microdomains whereas the poly(C8-STY) and poly(C12-STY) systems behave like classical polyelectrolytes.

Introduction

In solution, amphiphilic molecules (surfactants) spontaneously self-associate to give rise to a variety of structures having the characteristics of liquids (micelles, vesicles, microemulsions) or of liquid crystals (lyotropic phases such as lamellar or hexagonal) and of crystals (cubic phases). The capacity of the surfactant to form organized phases and its adsorption at interfaces are the basis of most practical uses of surfactants. Such organized assemblies are indeed extensively used in high added value applications most notably in the formulation of drugs and cosmetics and in the delivery of drugs. A problem facing these applications is the stability of the systems owing to their dynamic nature. For example, in micellar systems, monomer exchanges occur permanently between the micellar and bulk aqueous phases.[1]

It has recently been proposed to enhance the stability of these labile organized structures by polymerization. This can be achieved by the use of polymerizable surfactants. Considerable work has been performed so far on the polymerization of vesicles, monolayers, and multilayers, and this topic has been reviewed.[2–7] In contrast, there have been relatively few reports on the polymerization of aqueous micellar systems.[8–21] This is probably due to the fact that vesicles are characterized by lifetimes much longer than micellar aggregates, making easier the preservation of the structure. In the case of micelles, the question regarding whether the micellar structure is retained, altered, or destroyed upon polymerization is still a matter of controversy. A topological polymerization in which the polymer geometry corresponds to the initial micelle of monomeric surfactant involves a number of requirements not easily fulfilled,[22] and the results obtained in this field are often fragmentary and inconclusive. In particular, the effect of a fundamental parameter, the lifetime of the assembly, has been usually neglected or not properly considered. The organized structure should have a lifetime longer than the characteristic time for the polymerization (related to the reciprocal of the rate constant) in order to remain identical during the reaction. This case is observed with vesicles. On the contrary, micelles may exhibit lifetimes fairly short, as compared to the polymerization time scale, leading to final materials strongly different from the starting structures. The lifetime of surfactant organized assemblies is mainly governed by parameters such as the alkyl chain length, the temperature, the ionic strength, etc., while the polymerization rate mainly depends on the nature of the polymerizable group. In addition, the formation of an oligomeric radical in the micelle upon polymerization can affect quite considerably its lifetime.

In this series of papers, we present a detailed investigation of the polymerization of surface-active monomers, the *n*-alkyldimethyl(vinylbenzyl)ammonium chlorides, capable of forming micelles in aqueous solution. The alkyl chain length of the surfactants was varied from 8 to 16 carbon atoms. This allowed us to explore a large range of micelle lifetimes and to discuss the effect of the lifetime on the polymerization mechanism and on the products formed. For the first time, the micellar systems have been thoroughly characterized prior to *and* after polymerization by means of light scattering, viscometry, conductivity, spectrofluorimetry, and time-resolved fluorescence quenching. In part 2, a kinetic study of the photoinitiated polymerization of these surfactants provides some new insight into the polymerization mechanism.

Experimental Section

Materials. The polymerization was initiated by azobis(isobutyronitrile) (AIBN), which was recrystallized twice from ethanol. All reactants used for the preparation of the monomers were distilled under reduced pressure. The solvents were purified by distillation.

Synthesis. *n*-Alkyldimethyl(vinylbenzyl)ammonium chlorides, referred to as C*n*-STY with $n = 8, 12$, and 16, of the chemical formula

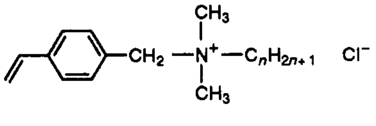

$$CH_2{=}CH{-}C_6H_4{-}CH_2{-}\overset{CH_3}{\underset{CH_3}{N^+}}{-}C_nH_{2n+1}\quad Cl^-$$

have been prepared by quaternization of the corresponding alkyldimethylamines (Ventron) with vinylbenzyl chloride (Tokyo Kasei). The C*n*-STY were purified by three recrystallizations from ethyl acetate in the presence of an inhibitor of polymer-

---

[*] To whom correspondence should be addressed.

[⊛] Abstract published in *Advance ACS Abstracts*, September 15, 1993.

0024-9297/93/2226-5755$04.00/0

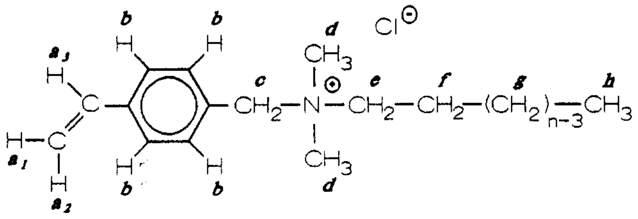

Figure 1. Assignment of the spectral lines observed for C*n*-STY surfactants (see Table I).

Table I. Chemical Shifts of ^{1}H NMR Spectral Lines Observed for the Surfactants (See Figure 1)

	chemical shift δ (ppm)									
surfactant	a_1	a_2	a_3	b	c	d	e	f	g	h
C16-STY	5.40	5.85	6.70	7.50	5.05	3.35	3.50	1.80	1.30	0.90
C12-STY	5.45	5.85	6.70	7.50	5.10	3.30	3.50	1.80	1.30	0.90
C8-STY	5.35	5.85	6.70	7.50	5.10	3.30	3.50	1.80	1.25	0.85

Table II. Absorption IR Bands Corresponding to Valence Vibrations (ν) and Deformation Vibrations (δ) Observed for the Surfactants

absorption frequency (cm^{-1})	bond	absorption frequency (cm^{-1})	bond
3020	ν_{CH} (aromatic)	1480	$\delta_{C=C}$ (aromatic)
2920	ν_{CH} (aliphatic)	910	δ_{CH} (aromatic)
2860	ν_{CH} (aliphatic)	840	δ_{CH} (aromatic)
1640	$\delta_{C=C}$ (aromatic)	740	δ_{CH} (aromatic)

Table III. Elemental Analysis of C*n*-STY Surfactants

		C	H	N	Cl	H_2O
C16-STY	% exp	76.49	11.71	3.02	8.33	1.88
	% calc	77.06	11.41	3.33	8.20	
C12-STY	% exp	75.26	11.33	3.62	9.61	0.77
	% calc	75.51	10.94	3.83	9.70	
C8-STY	% exp	69.39	10.39	4.07	11.77	1.60
	% calc	73.66	10.34	4.52	11.47	

ization, *tert*-butylcatechol (Aldrich), and dried under vacuum at room temperature. C8-STY was obtained as a slightly yellow paste.

Structure and Purity Control. The structure of the synthesized surfactants and their purity have been checked by ^{1}H NMR, IR spectroscopy, and microanalysis.

^{1}H NMR. The NMR spectra were recorded using a AC200 Bruker spectrometer. The solvent was deuterated chloroform ($CDCl_3$). Figure 1 and Table I give the assignments and chemical shifts δ (expressed in ppm units) of the different spectral lines observed for the three monomeric surfactants. The analysis of the different spectra allowed us to confirm the structure of the surfactants and to check that no polymerization occurred during their synthesis.

IR Spectroscopy. IR spectra were obtained by using a Perkin-Elmer 983 spectrophotometer with the solid surfactant dispersed into KBr pellets. Table II lists the bands obtained for the different surfactants and the corresponding bonds. The presence of the aromatic band vibrations ν_{CH} and aromatic deformations $\delta_{C=C}$ and δ_{CH} confirms the presence of a styryl group in the synthesized compounds.

Microanalysis. The weight percentages of C, H, N, and Cl from microanalysis are listed together with the theoretical values in Table III. The water content in the surfactant was measured by Karl Fischer titration using an automatic KFE452 titrimeter. The purity of the C16-STY and C12-STY compounds appears to be very good. That of the C8-STY is of about 96–98% on the basis of its C and Cl contents. A passage over a chromatography column using silica gel did not improve its purity.

Polymerization Procedure. Purified nitrogen was bubbled through the micellar solutions under stirring for about 30 min to eliminate oxygen in an apparatus similar to that described elsewhere,[23] before irradiation at 25 °C by a source of ultraviolet light (Philips; HPK 125) with AIBN as an oil-soluble initiator. The C*n*-STY surfactants are characterized in UV spectrophotometry by an absorption band at 250 nm. This feature allowed a direct measurement of the change of the degree of conversion of the monomer into polymer with time. A series of samples with variable characteristics has been prepared under these experimental conditions. As polymerization proceeds, the aspects of the C8-STY and C16-STY solutions become significantly different. The former remain optically transparent, but their viscosity increases progressively throughout the reaction. In contrast, the polymerization of the C16-STY solutions yields slightly bluish systems of low viscosity. After polymerization, the solution is freeze-dried. The resulting solid powder is solubilized in a small volume of a 50/50 (v/v) water/acetone mixture. This solution is then precipitated under stirring in a large excess of a 80/20 (v/v) ethyl acetate/acetone mixture. The polymer is recovered by filtration and dried under vacuum at 50 °C before characterization.

Static Light Scattering. The polymer molecular weights were determined by light scattering using dilute solutions in $CHCl_3$ or *n*-propanol/0.02 M or 0.05 M LiCl with an AMTEC SM 200 spectrophotometer. The optical source was a Siemens helium–neon laser operating at 632.8 nm.

The refractive index increments, d*n*/d*c*, were determined with a Brice-Phoenix differential refractometer operating at 632.8 nm and 20 °C.

Quasi-Elastic Light Scattering (QELS). This technique was used to determine the hydrodynamic radius of the polymers in dilute solution (1×10^{-4}–6×10^{-3} g·cm^{-3}) in *n*-propanol/0.02 M LiCl. Our apparatus used a Spectra Physics argon ion laser operating at 488 nm as the optical source. The time-dependent correlation function of the scattered intensity was obtained using a 72-channel digital correlator. The intensity correlation data were processed by using the cumulants method[24] to provide the average decay rate ⟨Γ⟩ and the variance ν of the autocorrelation function. The latter is a measure of the width of the distribution of decay rates and is given by

$$\nu = (\langle \Gamma^2 \rangle - \langle \Gamma \rangle^2)/\langle \Gamma \rangle^2 \qquad (1)$$

where $\langle \Gamma^2 \rangle$ is the second moment of the distribution. The translational diffusion coefficient D was determined from $\langle \Gamma \rangle$ according to:

$$\langle \Gamma \rangle = 2q^2 D \qquad (2)$$

where $q = 4\pi n \sin(\theta/2)/\lambda$ is the scattering vector; θ, the scattering angle; n, the refractive index of the continuous medium; and λ, the wavelength of the incident light. The diffusion coefficient in the high-dilution limit (surfactant concentration → cmc) is related to the hydrodynamic radius R_H of the particle according to the Stokes equation:

$$R_H = \lim\,(k_B T/6\pi\eta_0 D) \qquad (3)$$

where k_B is the Boltzmann constant; T, the absolute temperature; and η_0, the viscosity of the continuous medium.

Viscometry. The viscosity of rather dilute polymerized micellar solutions of C*n*-STY was measured at 25 °C with a low shear 30 Contraves viscometer (MS-LS 2T-2T) interfaced to a personal computer and driven by a software package supplied by the manufacturer.

Electrical Conductivity. An automated conductivity bridge (Wayne-Kerr B905) operating at 1 kHz and a conductivity cell (Tacussel CM02) have been used to measure the conductivity κ of aqueous solutions of C*n*-STY as a function of the surfactant concentration C. The breaks in the κ vs C plots and in the plot of the equivalent conductivity Λ vs $C^{1/2}$ yield the values of the critical micellar concentration (cmc) of the surfactants. Besides, the κ vs C plots provide an estimation of the micelle ionization degree, α.

Spectrofluorimetry. The fluorescence emission spectra of pyrene solubilized in aqueous solutions of C*n*-STY were recorded as a function of C using a Hitachi F-4010 spectrophotometer at an excitation wavelength of 335 nm. The ratio I_1/I_3 of the intensities of the first and third vibronic peaks in the emission spectrum of monomeric pyrene provides an estimate of the polarity sensed by pyrene it its environment.[25a] Besides, the change of I_1/I_3 with C provides the value of the cmc in the case of aqueous solutions of surfactant.[25a] Pyrenecarboxaldehyde has also been used. It is characterized by a maximum in the emission spectrum which occurs at a wavelength dependent on the medium polarity.[25b]

Time-Resolved Fluorescence Quenching (TRFQ). This method has been used to determine the micelle aggregation number of the C*n*-STY surfactants in aqueous solution and also to estimate the number of repeat units making up a hydrophobic microdomain in the polymerized micellar solutions of C16-STY (see below). This method rests on the analysis of the fluorescence decay curves (plots of the fluorescence intensity versus time after pulse excitation) recorded for solutions of amphiphiles where the micelles or the hydrophobic microdomains have solubilized a fluorescence probe and a quencher which are both sequestrated in the micelles.[26]

For each amphiphilic solution, two fluorescence decay curves are recorded, one in the absence of quencher and the other in the presence of quencher, such that $[Q]/[M] \simeq 1$ ($[Q]$ = quencher concentration, $[M]$ = micellar or microdomain concentration). In both instances $[P]/[M] < 0.05$ ($[P]$ = probe concentration). The equations

$$I(t) = I(0)\exp(-t/\tau) \qquad (4)$$

$$I(t) = I(0)\exp\{-A_2t - A_3[1-\exp(-A_4t)]\} \qquad (5)$$

are then fitted to the decay curves in the absence and presence of quencher. $I(t)$ and $I(0)$ are the fluorescence intensities at time t and time 0, and τ is the fluorescence lifetime of pyrene at its solubilization site. A_2, A_3, and A_4 are constants independent of time.

In the simple case where the probe and quencher distributions do not vary over a time long with respect to τ

$$A_2 = 1/\tau \qquad A_3 = [Q]/[M] \qquad A_4 = k_Q \qquad (6)$$

where k_Q is the rate constant for intramicellar quenching. The micelle aggregation number or the number of repeat units per microdomain N is given by:

$$N = A_3(C - C_f)/[Q] \qquad (7)$$

where C is the surfactant concentration or polymer concentration (expressed in moles of repeat units). C_f is the concentration of free amphiphile, that is the cmc or the concentration of repeat units not involved in forming microdomains. The difficulties involved in determining C_f in the case of polyamphiphile in solution have been discussed.[27] Besides, the microdomains appear to be polydisperse,[27] and this introduces an additional difficulty.[26d,e]

When the probe and quencher distribution vary during the probe lifetime, the expressions for A_2, A_3, and A_4 depend on the process by which the probe and quencher migrate from one micelle to another and include the pseudo-first-order rate constant k_m of this process.[26] The TRFQ method is then capable of providing information on the dynamics of the system investigated.

In all instances the TRFQ method works best when τk_Q is large. This is the reason why a water-insoluble probe with a long lifetime is generally used, as for instance pyrene ($\tau \simeq$ 300–400 ns in micellar solutions). Besides, efficient quenchers, that is, characterized by large k_Q values, are favored. In this work various probe–quencher pairs have been tested and used, depending on the system under investigation (see below).

Results and Discussion

1. Characterization of the Micellar Solutions. The micellar solutions prior to polymerization have been characterized by their critical micellar concentration (cmc) and their micelle aggregation number N. These two parameters have to be known with accuracy. Indeed, the cmc values are used as a guide for selection of the experimental conditions under which the polymerization is performed and for the interpretation of the results (see below). The values of N are critical for the understanding of the polymerization mechanism, since they are to be compared to the polymerization degrees of the polymers obtained from these micellar solutions.

Table IV. Cmc and Micelle Ionization Degrees for the C*n*-STY Surfactants from Conductivity and Fluorescence at 25 °C, in Pure Water

surfactant	cmc[a] (M)	cmc[b] (M)	α	cmc[c] (M)
C16-STY	2.9×10^{-4}	1.9×10^{-4}	0.323	2.5×10^{-4}
C12-STY	3.8×10^{-3}	3.6×10^{-3}	0.469	4.1×10^{-3}
C8-STY	8.8×10^{-2}	8.1×10^{-2}	0.349	

[a] Values from the κ vs C plots. [b] Values from the Λ vs $C^{1/2}$ plots. [c] Values from the I_1/I_3 vs C plots.

Table V. Probe–Quencher Pairs Used in TRFQ Studies of C*n*-STY Surfactants

surfactant	probe	quencher
C16-STY	$Ru(bipy)_2(bipy2C_{17})Cl_2$	hexadecyl-4-cyano-pyridinium chloride
C12-STY	$Ru(bipy)_2(bipy2C_{14})Cl_2$	tetradecyl-4-cyano-pyridinium chloride

1.1. Critical Micellar Concentration. The values of the cmc obtained by electrical conductivity and fluorescence probing are listed in Table IV, together with the micelle ionization degrees α deduced from conductivity experiments. A good agreement is observed between the three sets of values. These values obey the usual equation[28]

$$\log \text{cmc} = A - Bn \qquad (8)$$

where n is the number of carbon atoms in the surfactant alkyl chain and A and B are two constants for a homologous series of surfactants. The values of A (1.45) and B (0.316) for the C*n*-STY are close to those reported for the homologous series of nonpolymerizable cationic surfactants, the *n*-alkyltrimethylammonium chlorides ($A = 1.23$ and $B = 0.33$).[28]

A large difference was found between the values of the intensity I_1 of the first emission peak of pyrene measured in 10^{-3} M micellar solutions of C16-STY ($I_1 = 1.63$) and of its nonpolymerizable analogue, hexadecylbenzyldimethylammonium chloride ($I_1 = 6.70$). This difference is due to the strong quenching of the fluorescence emission of the micelle-solubilized pyrene by the $-CH{=}CH_2$ moiety of the styryl group of C16-STY, as already reported for other surfactants containing such a moiety.[29] This result is confirmed by the fluorescence lifetime measurements reported below. It suggests that the styryl groups are oriented toward the micelle hydrophobic core, so that the $-CH{=}CH_2$ groups come sufficiently close to the solubilized pyrene to quench its fluorescence. Thus, in this respect the C*n*-STY surfactants behave like two-chain quaternary ammonium surfactants. This is an important point which must have some bearing on the micellar behavior of C*n*-STY surfactants as well as their polymerization.

1.2. Aggregation Number. Since pyrene is quenched by the styryl groups, it cannot be used as a fluorescence probe in TRFQ experiments. It was replaced by the ruthenium(II) derivatives: $Ru(bipy)_2(bipy2Cn)^{2+}\ 2Cl^-$, where bipy stands for bipyridine and bipy2C*n* is a bipyridine on which have been covalently fixed two alkyl (C_{14} or C_{17}) chains in order to make it more hydrophobic (these compounds were gifts from Prof. M. Gratzel, EPFL, Lausanne, Switzerland). Tetradecyl- or hexadecyl-4-cyanopyridinium chloride was used as quencher. The lengths of the alkyl chains of the probe and quencher were adjusted to that of the surfactant as listed in Table V, in order to bring a minimal perturbation to the micelles. The results reported below concern only C12-STY and C16-STY because the probes and quenchers at our disposal brought too large a perturbation to the C8-STY micelles.

The analysis of the decay curves in the absence of quencher yielded fluorescence lifetime values $\tau = 550 \pm$

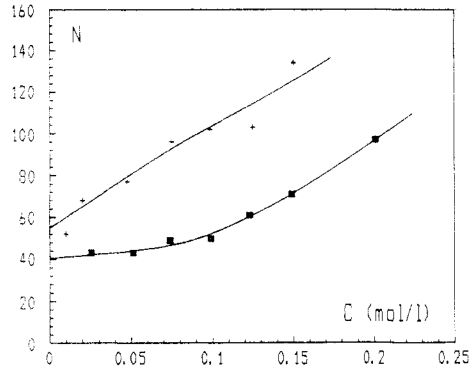

Figure 2. Variation of the micelle aggregation number N with the surfactant concentration for C12-STY (■) and C16-STY (+), in pure water.

10 ns, irrespective of the surfactant chain length and concentration. This indicates that the probe microenvironment is not dependent on these two parameters.

The analysis of the decay curves in the presence of quencher on the basis of eq 5 yielded values of A_2^{-1} close to those for τ, with C16-STY, indicating that there is no probe or quencher migration on the fluorescence time scale. For C12-STY, A_2^{-1} was found to be slightly smaller than τ, indicating that the probe and/or quencher used with this surfactant (see Table V) migrate(s) somewhat between micelles, via the bulk phase.[30] In this case the full expressions of A_2, A_3, and A_4 were used for the analysis of the data.[26] The values of the quantity τk_Q were found to be between 1 and 2 for the C12-STY micelles but between 1 and 0.6 for the C16-STY micelles as the surfactant concentration was increased from 0.01 to 0.15 M. It has been pointed out, on a theoretical basis, that the TRFQ method may not apply to systems where $\tau k_Q < 1$.[31,32] However, studies conducted in our laboratory on a given surfactant solution with probe–quencher pairs characterized by τk_Q values between 0.5 and 1 and above 1 yielded similar values of the micelle aggregation number, within experimental accuracy.[33] This led us to believe that the N values obtained for the C16-STY micelles are correct.

Figure 2 shows that for the two surfactants N increases with C, in the whole range of C for C16-STY but only above about 0.05 M for C12-STY. Thus the micelle growth becomes more important as the surfactant chain length increases. A similar result was reported for other series of homologous surfactants.[34]

It is of interest to compare the values of N at the cmc of the Cn-STY surfactants, obtained by extrapolation of the plots in Figure 2, to those calculated using the spherical oil drop model for the micelle hydrophobic core.[35] This model assumes the drop radius to be equal to the length l_c of the fully extended surfactant alkyl chain and excludes solvent penetration in the core. Using the reported expressions of l_c and of the volume v occupied by an alkyl chain in the micelle core,[36] in terms of the number n of carbon atoms in the alkyl chain, one can easily calculate the number N_s of alkyl chains per drop according to

$$N_s = 4\pi l_c^3/3v \qquad (9)$$

In the case of the Cn-STY surfactants, however, a difficulty arises because of the presence of the styryl group. Fluorescence intensity measurements showed that this group is preferentially located in the hydrophobic core (see above). This conclusion was confirmed by pyrene fluorescence lifetime measurements in micellar solutions of C16-STY and of its nonpolymerizable homologue, the hexadecyldimethylbenzylammonium chloride. The values τ = 69.5 and 360 ns, respectively, were obtained. Such a large difference can only be accounted for by a strong fluorescence quenching of pyrene by the C16-STY styryl group, thus confirming its partial localization in the micellar hydrophobic core.

Table VI. Values of l_c and v and of the Calculated (N_s) and Extrapolated to the cmc (N_0) Micelle Aggregation Numbers, in Pure Water

n	8	12	16	n	8	12	16
v (Å^3)	404	512	620	N_s	16	38	69
l_c (Å)	11.6	16.6	21.7	N_0		40	55

This fact led us to take into account the volume of the styryl group in calculating v. We assumed this group to roughly have a volume equivalent to that of six methylene groups. Table VI lists the values of v, l_c, and N_s and of N_0, the value of the aggregation number obtained by extrapolating the experimental data to the cmc. It is seen that the N_s values are rather low and in agreement with the N_0 values, in view of the assumptions involved. Note that similar calculations yield N_s = 27, 56, and 94 for n = 8, 12, and 16, respectively, when the styryl group is not accounted for. These values are much larger than the extrapolated ones, and the differences support, a posteriori, the localization of the styryl group in the micelle core.

The above results suggest that the Cn-STY micelles are spherical or spheroidal at low C. The increase of N with C implies that the micelles become increasingly anisotropic at higher concentration.

2. Polymerized Systems. Reports on the structure of polymerized micellar systems are scarce, obviously because the systems often phase separate or precipitate upon polymerization. In the present case, the polymerized systems remained stable and transparent or translucent, allowing their characterization by means of complementary techniques: spectrofluorimetry, viscometry, and TRFQ. Besides, the molecular weights and the dimensions of the polymers have been measured by static and dynamic light scattering. Cryotransmission electron microscopy has also been used to visualize the microstructure in the polymerized systems.[37]

2.1. Molecular Weights of the Polymers. The values of the molecular weights of the polymers obtained by polymerization of the Cn-STY micellar solutions are crucial as they can tell whether the initial micellar structure is retained upon polymerization. In this respect, the conclusions of the reported studies are often contradictory.[8,38] For surfactants containing a polymerizable group of low reactivity, as an allyl group, the polymer formed is often characterized by a degree of polymerization not too different from the micelle aggregation number before polymerization.[13,17,39] However, as noted by Hamid and Sherrington[22] and discussed in part 2, this can be fortuitous and most probably results from a facile monomer transfer reaction rather than from a topochemical polymerization.

On the contrary, surfactants containing a rather reactive polymerizable group (acrylamido, acrylate, ...) yield polymers of high molecular weight.[19,40,41] This excludes any possibility of intramicellar polymerization but rather implies intermicellar monomer exchanges in the course of the polymerization. The high cmc value of C8-STY (0.08 M) allowed us to carry out polymerization reactions above and below the cmc and, thus, to assess the effect of the micelle formation on the molecular weight of the poly(C8-STY) formed.

The results reported below concern mostly poly(C8-STY) and poly(C16-STY) as these two polymers represent two limiting situations (see part 2).

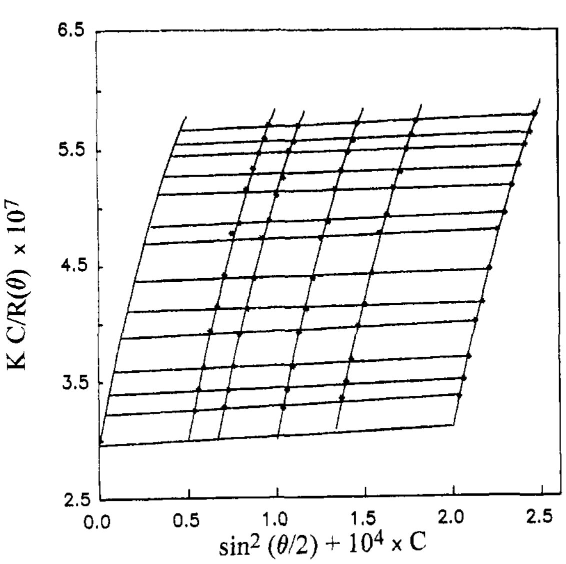

Figure 3. Example of the Zimm plot obtained for poly(C16-STY) in *n*-propanol/0.02 M LiCl.

Table VII. Values of the Refractive Index Increment for Poly(C8-STY) and Poly(C16-STY) in Various Solvents

solvent	d*n*/d*c* poly(C8-STY)	d*n*/d*c* poly(C16-STY)
$CHCl_3$	0.125	0.084
MeOH		0.223
LiCl (0.02 M)/*n*-propanol	0.165	0.142
LiCl (0.05 M)/*n*-propanol	0.168	0.142

Poly(C16-STY) was found to be soluble in a limited number of solvents: chloroform and alcohols. The solid poly(C16-STY) and poly(C12-STY) obtained by freeze drying from the optically clear or slightly bluish polymerized micellar solutions could not be resolubilized in water, contrary to poly(C8-STY). Such a behavior, already reported,[15,42,43] is attributed to the fact that, in the solid polymer, the ionic groups form clusters surrounded by hydrophobic chains which impede their access to water molecules.

2.1.1. Method of Measurement. Gel permeation chromatography (GPC) could not be used for the determination of the poly(C*n*-STY) molecular weight, because these cationic polymers are strongly adsorbed on the columns. Therefore, the weight-average molecular weights, $\overline{M}_w$, were measured by static light scattering. Table VII lists the values of the refractive index increment, d*n*/d*c*, obtained for poly(C16-STY) and poly(C8-STY) in different solvents. The relatively high value of the increment in methanol made this solvent look attractive. However, its polarity was still too high for a full screening of the electrostatic interactions, and addition of NaCl, in view of reducing these interactions, resulted in too low a solubility of poly(C16-STY). This led us to use a less polar alcohol. The *n*-propanol with 0.02–0.05 M LiCl was found to be a good compromise.

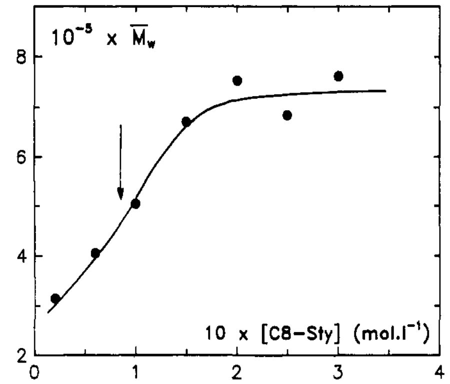

Figure 4. Variation of the poly(C8-STY) molecular weight with the initial surfactant concentration. The arrow indicates the cmc (from conductivity) in the presence of AIBN. [AIBN]/[C8-STY] = 0.78%.

Table VIII. Characteristics of Poly(C16-STY) and Poly(C8-STY) Samples in Various Solvents

	$10^{-6}\overline{M}_w$		$\langle R_G^2\rangle^{1/2}$ (Å)		10^5B (mol·cm^3·g^{-2})	
solvent	*a*	*b*	*a*	*b*	*a*	*b*
$CHCl_3$	3.38 ± 0.12	1.38 ± 0.69	810 ± 40	583 ± 11	6.53	12.2
n-propanol/ 0.02 M LiCl	3.39 ± 0.41	1.17 ± 0.63	738 ± 15	572 ± 21	4.04	19.4
n-propanol/ 0.50 M LiCl	3.28 ± 0.38	1.10 ± 0.55	745 ± 10	565 ± 11	4.04	17.2

[a] Poly(C16-STY). [b] Poly(C8-STY).

Table IX. Effect of the Initial C8-STY Concentration on the Characteristics of the Obtained Poly(C8-STY) Samples

N_{mic}	10[C8-STY] (M)	$10^{-5}\overline{M}_w$	$\langle R_G^2\rangle^{1/2}$ (Å)	10^4B (mol·cm^3·g^{-2})
	0.6	4.05 ± 0.49	417 ± 31	1.5
81	1.0	5.04 ± 0.68	454 ± 25	1.1
108	1.5	6.70 ± 0.78	570 ± 17	2.3
121	2.0	7.53 ± 0.88	555 ± 13	1.7
110	2.5	6.84 ± 0.83	545 ± 40	1.2
94	3.0	7.62 ± 0.82	560 ± 22	1.5

Table X. Effect of the Initial C16-STY Concentration on the Characteristics of the Obtained Poly(C16-STY) Samples

N_{mic}	10^2[C16-STY] (M)	$10^{-6}\overline{M}_w$	$\langle R_G^2\rangle^{1/2}$ (Å)	10^5B (mol·cm^3·g^{-2})
52	0.48	0.87 ± 0.10	472 ± 16	8.4
65	1.0	1.46 ± 0.18	519 ± 19	−6.8
80	2.0	2.15 ± 0.27	630 ± 24	−1.5
92	3.0	2.60 ± 0.32	643 ± 17	−3.7
105	4.8	3.39 ± 0.41	738 ± 15	0.4

In order to check the reliability of the measurements, the polymer characteristics, i.e., $\overline{M}_w$, radius of gyration $\langle R_G^2\rangle^{1/2}$, and second virial coefficient *B* of poly(C16-STY) and poly(C8-STY) samples, were measured both in chloroform and in *n*-propanol with 0.02 and 0.05 M LiCl. Figure 3 shows an example of Zimm plot. The polymer characteristics in the various solvents are listed in Table VIII. The agreement between the different sets of results is excellent, giving full confidence in the data. In the following *n*-propanol/0.02 M LiCl was systematically used as solvent for the determination of the $\overline{M}_w$ of the poly(C*n*-STY) samples.

2.1.2. Effect of the Initial C*n*-STY Concentration. This effect was studied at a molar ratio [initiator]/[monomer] = 0.78%.

The results relative to C8-STY and C16-STY are given in Tables IX and X, and the corresponding variations of $\overline{M}_w$ with the initial monomer concentration are represented in Figures 4 and 5. It can be seen that the micellar polymerization process leads to polymers of high molecular weights: 3×10^5–7×10^5 for C8-STY and 1×10^6–3×10^6 for C16-STY. These high $\overline{M}_w$ values clearly indicate that the micellar structure is not locked in by the polymerization since the degrees of polymerization range between 1×10^3 and 8×10^3 as compared to micelle aggregation numbers of 20 for C8-STY (based on results for ionic surfactants having the same alkyl chain)[44,45] and 55–80 for C16-STY before polymerization, in the concentration range inves-

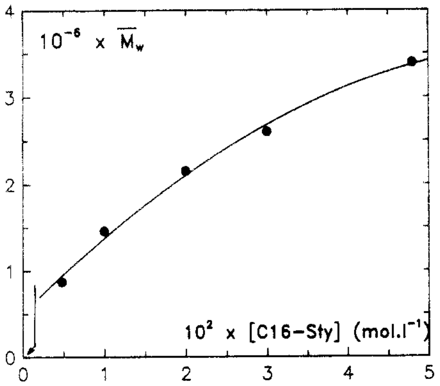

Figure 5. Variation of the poly(C16-STY) molecular weight with the initial surfactant concentration. Arrow: same meaning as in Figure 4. [AIBN]/[C16-STY] = 0.78%.

Table XI. Structural Characteristics of the Poly(C*n*-STY) Samples

polymer	[AIBN] (mM)	initial monomer concn (M)	$10^{-5}\overline{M}_w$	$\langle R_G^2\rangle^{1/2}$ (Å)	R_H (Å)	$\langle R_G^2\rangle^{1/2}/R_H$
poly(C8-STY)	1.47	0.0476	3.1 ± 0.2	272 ± 27	139 ± 10	1.95
poly(C16-STY)	3.40	0.15	21 ± 2.5	618 ± 13	292 ± 13	2.11

tigated (see Figure 2). Simple calculations indicate that the formation of a macromolecule requires the association of a number N_{mic} of micelles which ranges between 50 and 100 (Tables IX and X) depending on the surfactant and its initial concentration.

The following points can also be drawn out from the data:

(i) The polymer molecular weight increases with the initial concentration of micellized surfactant.

(ii) A rapid drop of $\overline{M}_w$ is observed for polymerization carried out at surfactant concentrations which encompass the cmc range (case of C8-STY, see Figure 4). This result is obviously caused by a mixed mechanism of homogeneous and heterogeneous polymerizations. Indeed, when the fraction of micellized surfactant is fairly low (at *C* only slightly above cmc), the homogeneous polymerization mechanism predominates, leading to the formation of relatively low molecular weight polymers, owing to the slower rate of polymerization which allows the occurrence of chain stoppage before large $\overline{M}_w$ values are reached. This point regarding the polymerization mechanism is fully discussed in part 2 of this work.

The values of the second virial coefficient *B* are positive for poly(C8-STY), whereas they are close to zero or slightly negative for poly(C16-STY). This indicates a somewhat less good solvent quality for the latter, probably due to its more pronounced hydrophobic character as compared to poly(C8-STY).

2.1.3. Conformational Behavior of Poly(C*n*-STY) in *n*-Propanol/0.02 M LiCl.

Quasi-elastic light scattering was used in conjunction with static light scattering to obtain such information. Recall that the former technique yields the hydrodynamic radius R_H of the polymer and the latter, its radius of gyration R_G. The ratio R_G/R_H depends on polymer morphology. For hard spheres, $R_G/R_H = 0.6^{1/2}$, whereas for a flexible macromolecular chain, R_G/R_H depends on the solvent quality. The theory of Akcasu and Han[46] predicts values of 1.506 in a θ-solvent and 1.862 in a good solvent.

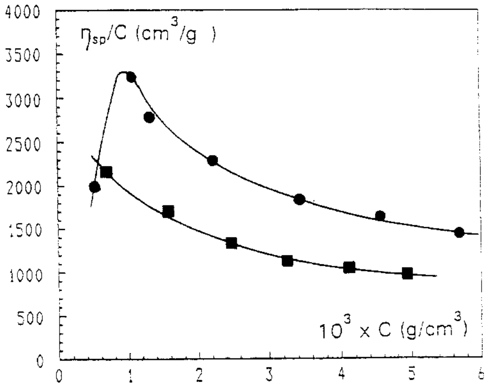

Figure 6. Variation of the reduced viscosity with the polymer concentration, of poly(C8-STY) (●) and poly(C12-STY) (■), in pure water.

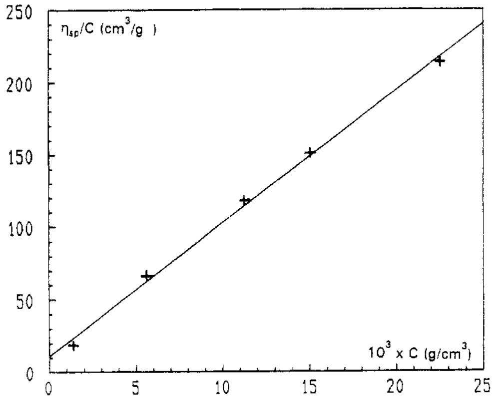

Figure 7. Variation of the reduced viscosity with the poly(C16-STY) concentration in pure water.

Table XII. Characteristics of the Polymerized Samples Used in Viscometric Studies

sample	10^4-[AIBN] (M)	initial monomer concn (M)	$10^{-6}\overline{M}_w$	$\langle R_G^2\rangle^{1/2}$ (Å)	10^5B (mol·cm^3·g^{-2})
poly(C8-STY)	7.50	0.10	1.52 ± 0.08	716 ± 18	14
poly(C12-STY)	7.80	0.10	0.71 ± 0.08	395 ± 16	3.7
poly(C16-STY)	1.09	0.14	2.60 ± 0.14	604 ± 19	1.7

The measurements were carried out on a single sample of poly(C8-STY) and of poly(C16-STY). The structural characteristics of the samples are given in Table XI. The values of R_G/R_H are close to the theoretical value and to experimental ones for flexible polymers in a good solvent.[47–49] This result confirms that poly(C16-STY) and poly(C8-STY) in solution in *n*-propanol/0.02 M LiCl behave as solvent-swollen coils.

2.2. Structure of the Systems after Polymerization.

We present below a study by means of several techniques of the structure and microstructure of the particles formed after polymerization of the aqueous micellar solutions as described above. The polymerized systems have been directly characterized after extensive dialysis against water in order to eliminate residual monomer and initiator. An important result of this investigation is that poly(C8-STY) and poly(C16-STY) show very different behaviors, corresponding to rather different microstructures.

2.2.1. Viscometric Study.

The initial surfactant concentration used in the preparation and the molecular characteristics of the polymers measured by light scattering are listed in Table XII. Figures 6 and 7 represent the variation of the reduced viscosity η_{sp}/C with the polymer concentration, *C*, in pure water for poly(C8-STY), poly(C12-STY), and poly(C16-STY). The behavior observed for the poly(C16-STY) is very different from that of the other two polymers. For the latter, the increase of η_{sp}/C upon decreasing *C* is typical of polyelectrolytes in an extended coil conformation. Besides, the curve relative

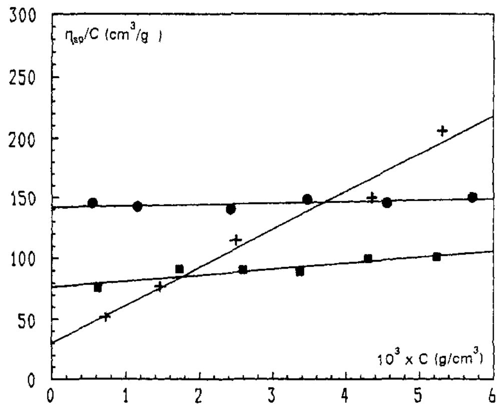

Figure 8. Variation of the reduced viscosity with the polymer concentration in 0.04 M NaCl aqueous solutions of poly(C8-STY) (●), poly(C12-STY) (■), and poly(C16-STY) (+).

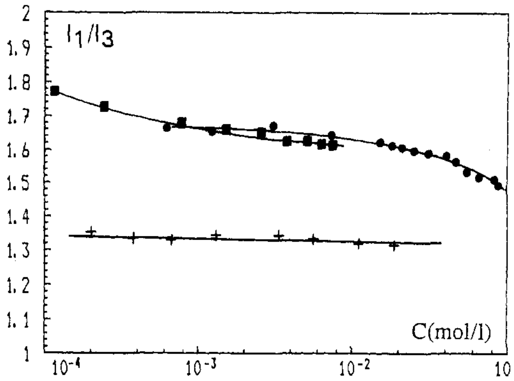

Figure 9. Variation of I_1/I_3 with the polymer concentration for poly(C8-STY) (●), poly(C12-STY) (■), and poly(C16-STY) (+) (λ_{exc} = 335 nm), in pure water.

to poly(C8-STY) exhibits a maximum. The decrease of η_{sp}/C at very low C is usually attributed to the presence of ionic impurities[50] (carbonic acid, for instance). At very low polymer concentrations, these impurities are capable of efficiently screening the electrostatic repulsions to give rise to this maximum. On the contrary, a linear increase of η_{sp}/C with C is seen for poly(C16-STY) with viscosities an order of magnitude smaller, suggesting a very compact conformation. The behavior of poly(C16-STY) is similar to that reported for polysoaps.[51,52]

To gain further insight into the conformation of the polymers, we have plotted the variations of $(\eta_{sp}/C)^{-1}$ with $C^{1/2}$ for the three samples. Indeed the Fuoss–Strauss equation derived for polyelectrolytes is[53]

$$(\eta_{sp}/C)^{-1} = \alpha + \beta C^{1/2} \tag{10}$$

where α and β are two constants. As expected, straight lines (not shown) were obtained for poly(C8-STY) and poly(C12-STY). The plot for poly(C16-STY), not represented, showed a marked curvature, as expected from the linear variation of η_{sp}/C with C in Figure 7.

Our results are similar to those reported by Strauss et al.[51,52] on poly(4-vinylpyridine) partially quaternized by alkyl bromides. These authors noted important changes in the copolymer conformation depending on the degree of quaternization and the length of the alkyl chain. Above a threshold value of this degree, the hydrophobic attractive interactions between alkyl chains dominate the electrostatic repulsions between pyridinium groups, leading to more compact particles of smaller size. However, the poly(vinylpyridine) sample partially quaternized by dodecyl bromide showed a polysoap-type (compact) conformation in contrast with the polyelectrolyte-type (extended) conformation adopted by poly(C12-STY). Likewise, in the poly(sodium maleate-*co*-alkyl vinyl ether), the homologue with a decyl side chain also adopted a compact conformation.[54,55] These results indicate, in agreement with recent theoretical calculations, that the "density" of side chains (number of side chains per number of carbon atoms on the polymer backbone) is a very important parameter in regards to the conformation adopted by the polyamphiphile.[56]

The effect of the poly(C*n*-STY) concentration on the viscosity of the solutions in 0.04 M NaCl has been investigated, and the results are represented in Figure 8. The plots of η_{sp}/C vs C are linear for the three polymers. Thus the salt added was sufficient for a complete screening of the electrostatic repulsions in the solutions poly(C8-STY) and poly(C12-STY). These two polymers now behave like simple uncharged polymers. The slope of the plots yields the Huggins parameter k_H which characterizes the solvent–polymer interactions. The value of k_H obtained for poly(C16-STY) is abnormally high (k_H = 48.9) compared to those found for the other two samples (k_H < 0.8). Similarly high values have been reported for poly(4-vinylpyridine) partially quaternized by long alkyl chains.[52] It has been claimed that these large k_H values are associated to polymer chains in a collapsed state.[57] Another, possibly complementary, explanation is that the poly(C16-STY) chains self-aggregate. Indeed we have noticed that poly(C16-STY) solutions are extremely sensitive to additions of salt.

2.2.2. Spectrofluorimetry. The experiments involved two probes: pyrene and pyrenecarboxaldehyde.

In Figure 9 are plotted the variations of the pyrene I_1/I_3 ratio with the polymer concentration. The data for poly(C8-STY) and poly(C12-STY) fall on a single curve. The values are high, much larger than those found for micellar solutions of C8-STY and C12-STY prior to polymerization, even at C as high as 0.1 M, that is, above the cmc of C8-STY. The I_1/I_3 values remain high in the whole C range but show a small decrease upon increasing C, which may indicate that some interaction between pyrene and the polymer is taking place, most likely with the alkyl side chains. Nevertheless, the results clearly indicate that no hydrophobic microdomains are present in solutions of poly(C8-STY) and poly(C12-STY). On the contrary, for poly(C16-STY), I_1/I_3 is nearly constant in the range 10^{-4}–2×10^{-2} M and its value (1.30–1.34) is close to that measured in micellar solutions of C16-STY, prior to polymerization ($\simeq$1.33). This result clearly demonstrates the existence of hydrophobic microdomains in poly(C16-STY) solutions but does not tell whether the microdomains are formed intra- or intermolecularly.

For poly(C16-STY) in the range 5×10^{-7}–1×10^{-4} M, I_1/I_3 shows a sigmoidal decrease upon increasing C (not shown), which reflects the partition of pyrene between water and the microdomains. Indeed at very low C (<10^{-6} M) pyrene remains in water in spite of its very high binding constant to the microdomains, simply because the volume fraction of microdomains is extremely small. Similar results have been found for other polyamphiphiles and are the topic of a detailed investigation.[58]

The results obtained with pyrenecarboxaldehyde are listed in Table XIII. λ_M is the wavelength corresponding to the maximum of fluorescence emission. The first part of the table lists values of λ_M in a series of alcohols. These values clearly show the increase of λ_M with the dielectric constant ϵ of the solvent and were used to prepare a calibration curve $\lambda_M = f(\epsilon)$. The second part of the table lists λ_M values in various micellar solutions and in the polymerized systems. The dielectric constant $\bar{\epsilon}$ sensed by

Table XIII. Values of λ_M for Pyrenecarboxaldehyde in Various Solvents and Amphiphilic Systems and of the Dielectric Constant of These Media[a]

solvent	ϵ	λ_M (nm)	micellar system	λ_M (nm)	$\bar{\epsilon}$
1-octanol	10.3	443	DTAC[b]	448.7	26
1-butanol	17.1	445	CTAC[c]	445.5	18
1-propanol	20.3	446.5	C8-STY	458.6	41
ethanol	24.3	447.8	C12-STY	455.2	38
methanol	32.6	451.8	C16-STY	451.7	31
glycerol	43.0	460.4	poly(C8-STY)	453.5	36
			poly(C12-STY)	453.8	36
			poly(C16-STY)	439.0	<10

[a] Pyrenecarboxaldehyde concentration = 2×10^{-6} M; $\lambda_{exc} = 356$ nm. [b] Dodecyltrimethylammonium chloride. [c] Hexadecyltrimethylammonium chloride.

pyrenecarboxaldehyde in these systems was obtained from the values of λ_M and the calibration curve. It should be emphasized[26f] that one should not compare the values of $\bar{\epsilon}$ in different micellar systems, where the probe may be at locations which are system-dependent. Only comparisons between homologous series are meaningful. The second part of Table XIII clearly shows that for micellar systems $\bar{\epsilon}$ decreases upon increasing chain length. Besides, the polarity sensed in poly(C16-STY) is much lower than in the other two polyamphiphiles, the difference being much too large when compared to the series of micellar systems, to reflect a simple decrease of $\bar{\epsilon}$ upon increasing alkyl chain length. This large difference is due to the existence of microdomains in poly(C16-STY), contrary to the other two polyamphiphiles.

2.2.3. Time-Resolved Fluorescence Quenching. This technique has been used to evaluate the aggregation number N (number of alkyl chains) of the hydrophobic microdomains present in poly(C16-STY) solutions. The method has been previously used for other polyamphiphiles with mixed success and still remains the only available one for obtaining this information.[27,59–61]

Since the polymerized systems contain no olefinic group, contrary to the monomeric ones, pyrene can be used as the fluorescence probe.

A series of quenchers of the pyrene fluorescence were tested, all of the surfactant type: tetradecyl- and hexadecylpyridinium and *p*-cyanopyridinium chlorides. These quenchers were found to work improperly; that is, the decay curves were not biphasic. The well-characterized high rigidity of the microdomains in solutions of polyamphiphiles[27,60] may be responsible for this behavior. Indeed, it may considerably hinder the incorporation of the quencher alkyl chain into the microdomains and give rise to a nonrandom distribution of quenchers among the microdomains. The electrostatic repulsions between the cationic quenchers used and the positively charged microdomains may also contribute to the observed behavior. This led us to use dibutylaniline (DBA) as the quencher because it is nonionic and has two short alkyl chains which need not penetrate deeply into the microdomains.

We first checked that the pyrene–DBA pair works properly by measuring the N values of DTAC and CTAC micelles using the pyrene–DBA and pyrene–tetradecylpyridinium pairs. The two sets of values agreed within experimental error. Besides, the pyrene fluorescence lifetime was found to have about the same value in the absence and presence of quencher. This result indicates that pyrene and DBA remain in the DTAC and CTAC micelles a long time compared to the fluorescence lifetime.[26]

Table XIV. Values of the Coefficients A_2, A_3, and A_4 in Equation 5 and of the Aggregation Number N of the Microdomains under Various Experimental Conditions

T (°C)	C (mM)	[DBA] (mM)	τ (ns)	A_2^{-1} (ns)	A_3	$10^{-6}A_4$ (s^{-1})	N
25.0	2.72	0.112	330	161	1.11	8.8	47
25.0	5.43	0.224	328	179	1.06	7.5	45
25.0	10.87	0.448	329	177	1.09	7.3	47
15.0	11.60	0.460	347	260	1.02	5.0	36
25.0	11.60	0.460	330	209	1.29	6.7	47
37.1	11.60	0.460	303	170	1.84	7.2	66
54.4	11.60	0.460	270	144	2.64	7.8	89

The pyrene decay curves for the pyrene–DBA pair in poly(C16-STY) solutions were analyzed using eqs 4 and 5, in the absence and presence of DBA, respectively, thereby providing the values of τ, A_2, A_3, and A_4. For all of the systems investigated, A_2^{-1} was found to be smaller than τ, indicating probe and/or quencher migration at the fluorescence time scale. Since migration did not take place in DTAC and CTAC solutions, one is led to assign this process to the hydrophobic microdomains. Migration was also observed in solutions of the polysoap PS16 [poly(disodium maleate-*co*-hexadecyl vinyl ether)].[27,55] The mechanism responsible for this effect is discussed below. The aggregation numbers N for the microdomains were calculated using the full expressions of A_2, A_3, and A_4[26,62] and assuming $C_f = 0$ in eq 7.[27] Because of this assumption the N values calculated represent upper bound values. Table XIV lists the values of N obtained under various experimental conditions. It is seen that N is independent of the polymer concentration and increases with T. This last result is unexpected (although it has been also reported for the polysoap PS16[27]), and we have tried to obtain supporting evidence by studying the effect of temperature on the fluorescence emission of pyrene. Indeed at fairly high pyrene concentration ($\simeq 10^{-4}$ M) the emission spectrum of pyrene shows a broad emission band centered around 480 nm, arising from pyrene excimers (dimers made of a pyrene in the excited state and a pyrene in the ground state). In homogeneous solutions the excimer fluorescence decreases because the excimers dissociate upon increasing temperature. In micellar solutions the pyrene is located in the micelles and the probability of excimer formation and, thus, the excimer fluorescence intensity I_E increase with the molar concentration ratio [pyrene]/[micelle] $\simeq$ N[pyrene]/[micellized surfactant]. At constant [pyrene], I_E will increase with N. In systems where N increases rapidly with T, the associated increase of I_E with T may compensate the normal decrease of I_E upon increasing T. This is exactly what we observed experimentally, with I_E remaining nearly constant or slightly increasing as the temperature was raised from 15 to 65 °C, as for the polysoap PS16.[55] This result confirms the increase of N with T. Recall that the aggregation number of ionic micelles has consistently been found to decrease upon increasing T.[63] Thus the microdomains in poly(C16-STY) solutions behave rather like micelles of nonionic surfactants for which N increases with T.[64] The unexpected behavior of poly(C16-STY) may arise from the increased conformational mobility of the polymer backbone with temperature, which may facilitate the self-association of the side chains.[27]

The results in Table XIV show a small increase of A_4 and, thus, of the rate constant k_Q with T. Recall that k_Q increases with T in micelles of ionic surfactants because both N and the microviscosity of the micelle interior decrease upon increasing T.[63] For the microdomains in poly(C16-STY) solutions, however, N increases with T and this effect nearly compensates the accompanying decrease of microviscosity, resulting in the observed small change of k_Q.

The various results reported above are very similar to those for the polysoap PS16,[27] and we are thus led to adopt the same model for the microstructure of poly(C16-STY) macromolecules. This model is that of a string of microdomains where the conformation of the polymer backbone may be locally ordered, forming short helices,[56] or more disordered, simply forming loops, with the side chains "inside" and the ionic headgroup coating these microdomains. Short polymer segments where the alkyl chains are not organized would connect the microdomains. Indeed cryotransmission electron microscopy visualized the individual macromolecules of poly(C16-STY) in an aqueous solution under the form of threadlike micelles.[37] Had the microdomains been far apart (long connecting segments) the electron micrographs would have shown globular micelles.

As discussed for the polysoap PS16,[27] the shortness of the segments connecting the successive microdomains probably explains the rapid exchange of probe and/or quencher between microdomains detected by TRFQ. Indeed the reactants need not migrate from one microdomain to another via the aqueous phase. This migration can take place by diffusion along the short connecting segments which are rather hydrophobic. Another possibility of migration is by "hoping" of reactants upon collision or contact between microdomains.

The value of N found for poly(C16-STY), slightly below 50 at 25 °C, is smaller than that of PS16, i.e., 60, and also somewhat smaller than that found for the C16-STY micelles. Nevertheless, the values of N found in poly(C16-STY) and C16-STY are not very different. At first sight, if measurements of molecular weights had not been performed on poly(C16-STY), one may have tentatively concluded that the (C16-STY) micelles are affected only little by the polymerization. Our data clearly show that a full characterization of the systems before and after polymerization, by many different techniques, sensitive to various properties is necessary in order to reach safe conclusions.

The present study did not address the question of microdomain size polydispersity. However, it is likely that, as for PS16,[27] the microdomains in poly(C16-STY) solutions are highly polydisperse.

Conclusions

Our main purpose in this study was to compare the properties (mainly the aggregate size characterized by its aggregation number) of micellar solutions of polymerizable surfactants to those of the same systems after photochemical polymerization of the surfactants.

We thus synthesized three polymerizable surfactants: the alkyldimethyl(vinylbenzyl)ammonium chlorides (Cn-STY with n = 8, 12 and 16). The cmc, micelle ionization degrees, and aggregation numbers of these surfactants were determined in aqueous solution. These surfactants were then photochemically polymerized in aqueous micellar solution, and the particles present in the system were characterized by various techniques. Light scattering showed that the degrees of polymerization of the polymers formed were much larger than the aggregation number of the micelles before polymerization. This result excludes a topochemical polymerization of the reactive monomers used and implies extensive exchange of material between micelles as polymerization proceeds. The microstructure of the aqueous solutions of poly(Cn-STY) was investigated by viscometry and fluorescence probing. Hydrophobic microdomains were found to be present in solutions of poly(C16-STY) which adopt a compact conformation. Microdomains do not form in solutions of poly(C8-STY) and poly(C12-STY) which adopt extended conformations, of the polyelectrolyte type.

Further studies of poly(C16-STY) by time-resolved fluorescence quenching provided upper bound values of the average number of repeat units per hydrophobic microdomain. The results indicated that the formation of microdomains is hindered by the polymer backbone and occurs mainly within the same polymer molecule. Also in a given polymer chain the successive microdomains appear to be close to each other, to the point of allowing a fast migration of solubilized reactants from one microdomain to another. Overall, the results obtained for poly(C16-STY) are very similar to those previously reported for another polyamphiphile: the poly(disodium maleate-*co*-hexadecyl vinyl ether).[27,55] At last, the comparison between the present results and those for another series of polyamphiphiles evidenced the extreme importance of the density of the alkyl side chains on the capacity of polyamphiphiles to form hydrophobic microdomains. This result supports recent theoretical calculations on the microstructure of polyamphiphiles in solution.[56]

Acknowledgment. The authors gratefully acknowledge the financial support of Rhône-Poulenc Co. during the whole course of this study.

References and Notes

(1) Lang, J.; Zana, R. In *Surfactant Solutions: New Methods of Investigation*; Zana, R., Ed.; Marcel Dekker: New York and Bäsel, 1986; Chapter 8, p 405.
(2) Fendler, J.H. In *Surfactants in Solution*; Mittal, K. L., Lindmann, B., Eds.; Plenum Press: New York, 1983; Vol. 3, p 1947.
(3) Pons, M.; Johnston, D. S.; Chapman, D. *J. Polym. Sci., Polym. Chem.* **1982**, *20*, 513.
(4) Bolikal, D.; Regen, S. L. *Macromolecules* **1984**, *17*, 1287.
(5) Gros, L.; Ringsdorf, H.; Schupp, H. *Angew. Chem., Int. Ed. Engl.* **1981**, *20*, 305.
(6) Ringsdorf, H.; Schlarb, B.; Venzmer, J. *Angew. Chem., Int. Ed. Engl.* **1988**, *27*, 113.
(7) Ringsdorf, H.; Schlarb, B.; Tyminski, P. N.; O'Brien, D. F. *Macromolecules* **1988**, *21*, 671.
(8) Paleos, C. M.; Malliaris, A. *J. Macromol. Sci., Rev. Macromol. Chem. Phys.* **1988**, *C28*, 403.
(9) Kammer, U.; Elias, H. G. *Kolloid Z. Z. Polym.* **1972**, *250*, 344.
(10) Sprague, E. D.; Duecker, D. C.; Larrabee, C. E. *J. Am. Chem. Soc.* **1981**, *103*, 6797.
(11) Arai, K.; Maseki, Y.; Ogiwara, Y. *Makromol. Chem., Rapid Commun.* **1987**, *8*, 563.
(12) Yeoh, K. W.; Chew, C. M.; Gan, L. M.; Koh, L. L. *J. Macromol. Sci., Chem.* **1989**, *A26*, 663.
(13) Paleos, C. M.; Dais, P.; Malliaris, A. *J. Polym. Sci., Polym. Chem. Ed.* **1984**, *22*, 3383.
(14) Nagai, K.; Ohishi, Y.; Inaba, M.; Kudo, S. *J. Polym. Sci., Polym. Chem. Ed.* **1985**, *23*, 1221.
(15) Hamid, S. M.; Sherrington, D. C. *Polymer* **1987**, *28*, 325, 332.
(16) Lerebours, B.; Perly, B.; Pileni, M. P. *Chem. Phys. Lett.* **1988**, *147*, 503.
(17) Durairaj, B.; Blum, F. D. *Langmuir* **1989**, *5*, 370.
(18) Chu, D. Y.; Thomas, J. K. *Macromolecules* **1991**, *24*, 2212.
(19) Ito, K.; Tanaka, K.; Tanaka, H.; Imai, G.; Kawaguchi, S.; Itsuno, S. *Macromolecules* **1991**, *24*, 2348.
(20) Laschewsky, A.; Zerbe, I. *Polymer* **1991**, *32*, 2070, 2081.
(21) Cochin, D.; Zana, R.; Candau, F. *Polym. Int.* **1993**, *30*, 491.
(22) Hamid, S.; Sherrington, D. *J. Chem. Soc., Chem. Commun.* **1986**, *936*.
(23) Hoorspool, W. M. *Aspects of Organic Photochemistry*; Academic Press: New York, 1976; p 42.
(24) *Photon Correlation and Light Beating Spectroscopy*; Cummins, H. Z., Pike, E. R., Eds.; Plenum Press: New York, 1974.
(25) (a) Kalyanasundaram, K.; Thomas, J. K. *J. Am. Chem. Soc.* **1977**, *99*, 209; (b) *J. Phys. Chem.* **1977**, *81*, 2176.
(26) (a) Infelta, P.; Gratzel, M.; Thomas, J. K. *J. Phys. Chem.* **1974**, *78*, 190. (b) Infelta, P. *Chem. Phys. Lett.* **1979**, *61*, 88. (c) Yekta, A.; Aikawa, M.; Turro, N. J. *Chem. Phys. Lett.* **1979**, *65*, 543. (d) Almgren, M.; Lofröth, J.-C. *J. Chem. Phys.* **1982**, *76*, 2734.

(e) Warr, G. C.; Grieser, F. *J. Chem. Soc., Faraday Trans. 1* **1986**, *82*, 813. (f) Zana, R. In *Surfactant Solutions: New Methods of Investigation*; Zana, R., Ed.; Plenum Press: New York, 1987; Chapter 5.

(27) Binana-Limbélé, W.; Zana, R. *Macromolecules* **1990**, *23*, 2731.

(28) Bourrel, M.; Schechter, R. S. *Microemulsions and Related Systems*; Marcel Dekker: New York, 1988; Vol. 30, p 46.

(29) Encinas, M.; Guzman, E.; Lissi, E. *J. Phys. Chem.* **1983**, *87*, 4770.

(30) Indeed both the probe and quencher used with C12-STY micelles have shorter alkyl chains than for C16-STY, and therefore their residence times in the micelles are shorter by a factor of about 10. This is sufficient to explain the observed slow exchange on the fluorescence time scale.

(31) Almgren, M.; Alsins, J.; Mukhtar, E.; van Stam, J. *J. Phys. Chem.* **1988**, *92*, 4479.

(32) Van der Auweraer, M.; Reekmans, S.; Boens, N.; De Schryver, F. C. *Chem. Phys.* **1989**, *132*, 91.

(33) Alami, E.; Van Os, N. M.; Ruppert, L.; De Jong, B.; Kerkhof, F. J.; Zana, R. *J. Colloid Interface Sci.* **1993**, *160*, in press.

(34) Lianos, P.; Lang, J.; Zana, R. *J. Colloid Interface Sci.* **1986**, *110*, 237. Lianos, P.; Zana, R. *J. Colloid Interface Sci.* **1981**, *84*, 100.

(35) Tartar, H. V. *J. Phys. Chem.* **1955**, *59*, 1195; *J. Colloid Interface Sci.* **1959**, *14*, 115.

(36) Tanford, C. *J. Phys. Chem.* **1972**, *76*, 3020.

(37) Cochin, D.; Candau, F.; Zana, R.; Talmon, Y. *Macromolecules* **1992**, *25*, 4220.

(38) Nagai, K.; Elias, H. G. *Makromol. Chem.* **1987**, *188*, 1095.

(39) Larrabee, C. E., Jr.; Sprague, E. D. *J. Colloid Interface Sci.* **1986**, *114*, 256.

(40) Yeoh, K. W.; Chew, C. H.; Gan, L. M.; Koh, L. L. *Macromol. Sci. Chem.* **1990**, *A27*, 63.

(41) Nagai, K.; Ohishi, Y. *J. Polym. Sci., Polym. Chem.* **1987**, *25*, 1.

(42) Larrabee, C. E.; Sprague, E. D. *J. Polym. Sci., Polym. Lett. Ed.* **1979**, *17*, 749.

(43) Salamone, J. C.; Israel, S. C.; Taylor, P.; Snider, B. *Polymer* **1973**, *14*, 639.

(44) Zemb, T.; Drifford, M.; Hayoun, M.; Jehan, A. *J. Phys. Chem.* **1983**, *87*, 4254.

(45) Hayter, J. B.; Zemb, T. *Chem. Phys. Lett.* **1982**, *93*, 91.

(46) Akcasu, A. Z.; Han, C. C. *Macromolecules* **1979**, *12*, 276.

(47) Selser, J. C. *Macromolecules* **1981**, *14*, 346.

(48) Meyerhoff, G.; Appelt, B. *Macromolecules* **1979**, *12*, 968.

(49) Nox, T.; Chu, B. *Macromolecules* **1979**, *12*, 1122.

(50) Lovel, P. A. In *Comprehensive Polymer Science*; Booth, C., Price, C., Eds.; Pergamon Press: New York, 1989; Vol. 1, Chapter 9, p 173.

(51) Strauss, U. P.; Gershfeld, N. L.; Crook, E. M. *J. Phys. Chem.* **1954**, *58*, 747.

(52) Strauss, U. P.; Gershfeld, N. L. *J. Phys. Chem.* **1956**, *60*, 577.

(53) Fuoss, R. M.; Strauss, U. P. *J. Polym. Sci.* **1948**, *3*, 246.

(54) Pefferkorn, E.; Schmitt, A.; Varoqui, R. *C. R. Acad. Sci. (Paris)* **1986**, *267*, 349.

(55) Binana-Limbélé, W.; Zana, R. *Macromolecules* **1987**, *20*, 1331.

(56) Turner, M. S.; Joanny, J. F. *J. Phys. Chem.* **1993**, *97*, 4825.

(57) Inoue, H. *Kolloid Z. Z. Polym.* **1964**, *195*, 102.

(58) Anthony, O.; Lang, J.; Zana, R., manuscript in preparation.

(59) Chu, D. Y.; Thomas, J. K. *J. Am. Chem. Soc.* **1986**, *108*, 6270.

(60) Chu, D. Y.; Thomas, J. K. *Macromolecules* **1987**, *20*, 2133.

(61) Hsu, J. L.; Strauss, U. P. *J. Phys. Chem.* **1987**, *91*, 6238.

(62) Roelants, E.; Geladé, E.; Van der Auweraer, M.; Croonen, Y.; De Schryver, F. C. *J. Colloid Interface Sci.* **1983**, *96*, 288.

(63) Malliaris, A.; Le Moigne, J.; Sturm, J.; Zana, R. *J. Phys. Chem.* **1985**, *89*, 2709.

(64) Zana, R.; Weill, C. *J. Phys. Lett. (Paris)* **1985**, *46*, 743.